# Polymer Electrostatics: Detection and Speciation of Trapped Electric Charges by Electric Probe and Analytical Electron Microscopy

*Fernando Galembeck, Carlos Alberto Paula Leite, Maria do Carmo V. M. da Silva, Amauri José Keslarek, Carlos Alberto Rodrigues Costa, Érico Teixeira-Neto, Márcia Maria Rippel, Melissa Braga*

Instituto de Química, Universidade Estadual de Campinas, PO Box 6154, Campinas SP, Brazil

**Summary:** This work reviews new probe and electron microscopy approaches for the detection of charged domains in insulating polymers, as well as for the identification of the charge-bearing species: scanning electric potential microscopy (SEPM), electric force microscopy (EFM) and energy-loss spectroscopy imaging in the transmission electron microscope (ESI-TEM). The SEPM and EFM micrographs show patterned domains bearing excess electric charges and extending for tens of nanometers, in polymer latex particles and films. The charged species are identified by ESI-TEM as emulsion polymerization initiator and surfactant residues, as well as the associated counter-ions. Charged domains are also observed in common thermoplastic polymers, producing unexpectedly large electric potential gradients.

## Introduction

Polymer dielectrics are usually described as electro-neutral solids, even though there is plenty of evidence showing that they contain domains with excess electric charges. Several phenomena related to the existence of fixed charges or polarization in polymers are described in the literature: their ability to acquire charges by friction, the formation of electrets, space and residual charges, double-layers at interfaces and interfacial polarization, which were shortly reviewed in a recent paper.[1] However, there is a conceptual constraint in dealing with these problems, that is the current idea of charge neutrality as a normal state for polymer dielectrics at every relevant length scale, from the macromolecules up to the macroscopic plastic solids (films, coatings, tubes) and devices. Of course, the prevalence of electroneutrality in any physical medium suggests that the ionic species carrying opposite charges should occupy neighboring sites and they should also move simultaneously.[2] A

 CCC 1022-1360/00/$ 17.50+.50/0

review article on the non-linear optical polymer electrets acknowledges that a corona discharge produces and carries chemically active species, which tend to attack and modify the surface and subsurface layers of organic materials. However, the spatial distribution and chemical identity of the resulting charge species responsible for polymer polarization was not described.[3] Other authors acknowledge the existence of ionic carriers in insulating polymers, but these have not yet been identified or located.[4]

These difficulties have not prevented the use of thermally stimulated discharge currents in polymers, in the study of polymer relaxations,[5,6,7] as well as the recognition of the formation of double-layers of opposite electrical charges by two dielectric contacting phases.[8,9]

Indeed, the formation of an electrical double layer at an interface is expected, considering the differences of dielectric constant between the two adjoining phases. Since most crystalline polymers are indeed multiphase systems, they should intrinsically display internal charge separation, due to the Maxwell and the Costa Ribeiro[10,11] effects. This idea is further supported by evidences[12] showing that the crystalline-amorphous interface plays an important role not only as a charge-trapping site but also in carrying an important amount of the total polarization in PVDF. The differences in dielectric constants of *e.g.* crystalline and amorphous domains in polyethylene (and other partially crystalline thermoplastics) are probably small, but their electronic polarization component is sufficient to impair the transparency of the partially crystalline polymer.

Beyond the differences of dielectric constant between amorphous and crystalline polymer domains, there are other factors that influence the formation of differentiated domains within a polymer: oxidized polymer chains can be segregated, as well as the immiscible catalyst residues and contaminants introduced during the fabrication of polymer and artifacts. Polymers prepared by emulsion polymerization or processed in polar media should always be contaminated with trapped ions, and these are not necessarily arranged in electro-neutral ion pairs or clusters.

However, there is also a prevailing but unproven idea, following which the charge-bearing species in neutral solids are found in ion pairs or clusters and thus they do not generate any effects at larger distances. This idea is largely due to a major experimental limitation, namely the difficulty to determine the existence of ionic species within insulating solids.

This difficulty is being overcome with the development of new techniques for electric potential or force mapping across solid surfaces, using a variety of scanning probe microscopies, appropriate for sensing charges,[13] dielectric constants, film thickness of insulating layers, photo-voltage and electric potentials.[14, 15]

Excess charges are necessarily associated with ionic species or free electrons, but charge speciation in dielectrics is also a challenging, largely unsolved problem of condensed matter physics and chemistry, even in the seemingly simpler case of liquid dielectrics.[16] This problem is addressed using an analytical electron microscopy; the method of choice is electron energy-loss spectroscopy associated to transmission electron microscopy (ESI-TEM), due to the high sensitivity coupled to a sub-nanometer spatial resolution. The present work reviews the application of microscopy to the detection of domains with excess electric charges, in insulating polymers.

## Probe microscopy for electric domain mapping: SEPM and EFM

Scanning electric potential microscopy (SEPM) images are acquired using the standard non-contact AFM set-up (in this case, a Topometrix Discoverer instrument) but with the following modifications: the probe tip is coated with Pt and it is fed with an AC signal, 10 kHz below the frequency of the normal AFM oscillator, which matches the natural frequency of mechanical oscillation of the cantilever-tip system (40-70 kHz). During a measurement, the mechanical oscillation of the tip is tracked by the four-quadrant photodetector and analyzed by two feedback loops. The first one is used in the conventional way to control the distance between tip and sample surface, while scanning the sample at constant oscillation amplitude. The second loop is used to minimize the electric field between tip and sample: a second lock-in amplifier measures the tip vibration at the AC frequency oscillation while scanning, and adds a DC bias to the tip, to recover the undisturbed AC oscillation. This technique differs from that used by Terris,[10] who measured the phase displacement of the AC voltage while in the Topometrix set up the phase displacement is cancelled by DC biasing. The image is built up by using the DC voltage fed to the tip, at every pixel, thus detecting electric potential gradients throughout the scanned area. This technique derives from the Kelvin bridge and it is reminiscent of the oscillating electrode method for monolayer study: both use an oscillating electrode

separated from the sample by an air gap. The main difference between them is the detection technique used, since SEPM uses a phase detection of the voltage applied.

The electric force microscopy (EFM)[17] technique uses a different approach: the surface is scanned at two different constant heights, typically 10 and 70 nm. In the first case, the interaction between tip and sample is determined by the short-range van der Waals forces, but at 70 nm the interaction is dominated by the electrostatic interactions. This technique is easily performed, but the results are not interpreted as unequivocally as the SEPM data.

A typical SEPM result is presented together with an AFM image of the same sample area in Figure 1, for a polystyrene latex. This was prepared by emulsion polymerization initiated with $K_2S_2O$ in the presence of a mixture of polyoxyethylene-23-lauryl ether and sodium dodecylsulfate surfactants.[18]

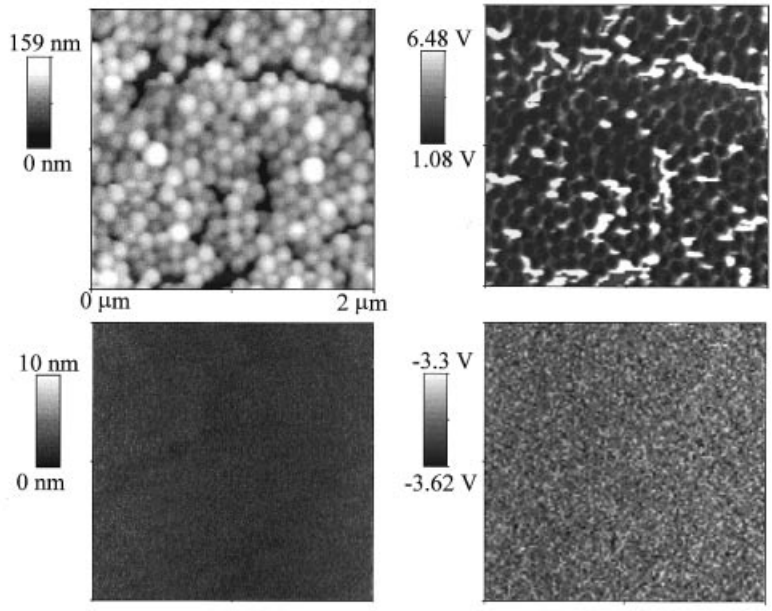


Figure 1. SEPM (right) and AFM (left) images of PS latex films on mica. On top are the figures of the as-prepared dry particles, and on the bottom is the film resulting from exposure of a dry film to a chloroform-saturated atmosphere, for 12 hours.

Another pair of AFM and SEPM images in the same figure show a film of the same latex,

but after exposure to an atmosphere saturated with chloroform.

Due to the polystyrene high $T_g$, the particles do not coalesce in the dry film; their cores are negative relative to the outer shells and to the inter-particle spaces, where the (positive) counter-ions are expected to accumulate. The observed potential differences exceed 5 volts, corresponding to large potential gradients. Following exposure to chloroform, the film appears very flat (maximum height difference is 10 nanometers in the area shown) and the observed potential differences are much smaller, less than 0.5 V but still larger than the zeta potential for this latex, which is -29 mV. [19]

AFM and SEPM images for a film of a low $T_g$ (15°C) poly(styrene-butyl acrylate-acrylic acid) latex prepared using redox initiation and sodium phenylether phosphate surfactant [20] have some unexpected features, as shown in Figure 2. Due to its low $T_g$ value, films cast from this latex are transparent, suggesting that particles are very well coalesced. However, particle borders are easily seen, both in the AFM and SEPM images.

This charge pattern is similar to that of the natural rubber latex (NRL) film in Figure 3: NRL also forms transparent films at room temperature, but particle individuality is easily observed at the film surface, even though the $T_g$ of cis(polyisoprene) is very low.

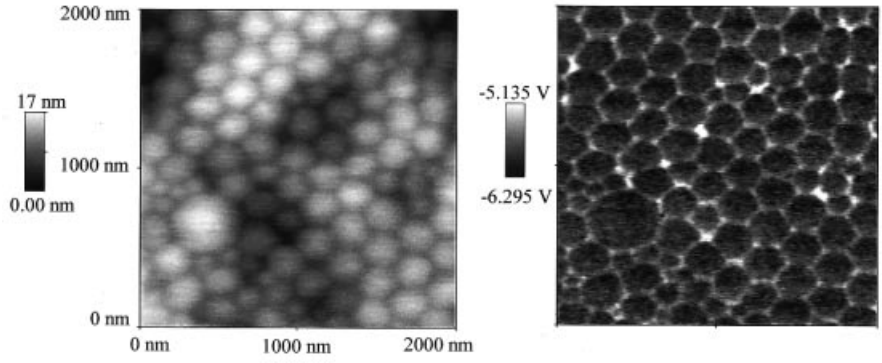


Figure 2. AFM and SEPM images of a transparent (transmittance>99%) copolymer (styrene-butyl acrylate-acrylic acid) latex film.

Consequently, there is a limit to inter-particle diffusion, and this is likely due to the particle shells with a different chemical composition from the particle bulk as evidenced by the

large positive electric potential, observed in the SEPM picture in Figure 3.

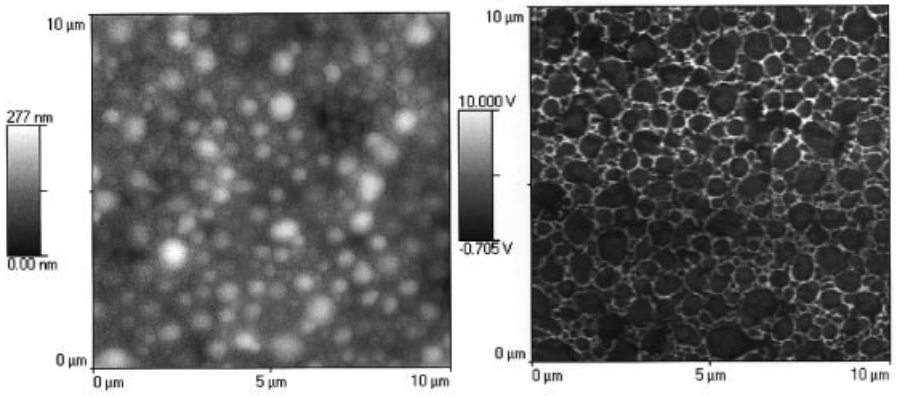


Figure 3. Non-contact AFM and SEPM maps of a natural rubber latex film, cast from freshly collected, centrifuged latex.

All these images have to be examined considering that the electrostatic interactions are long-range. This means, charges buried beneath the sample surface for tens and even a few hundred nanometers are detectable, but their contribution to the measured potentials decreases with the square of their distance to the scanning probe. In the case of the latexes, the observed electric potential gradients can be assigned to a spatial separation between anions (arising *e.g.* from the persulfate initiators or from anionic surfactants) and the corresponding counter-cations.

## Analytical electron microscopy: ESI-TEM

The elemental distribution within fine latex particles and thin films can be observed using the electron spectroscopy imaging technique, in a transmission electron microscope (ESI-TEM). A Carl Zeiss CEM 902 transmission electron microscope, equipped with a Castaing-Henry-Ottensmeyer energy filter spectrometer within the column was used. The spectrometer exploits inelastic scattered electrons to form element-specific images. When the electron beam passes through the sample, interaction with electrons of different elements results in characteristic energy losses. A prism-mirror system deflects electrons

with different energies to different angles so that only electrons with a well-defined energy are selected. If elastic electrons are the only chosen ($\Delta E = 0$ eV) a transmission image with reduced chromatic aberration is obtained. When monochromatic inelastic scattered electrons are selected, electron spectroscopy images (ESI) are formed, in which contrast is dependent on the local concentration fluctuations of a particular chosen element. Clear areas correspond to element-rich domains.

Examination of individual latex particles is possible, provided they are sufficiently small, or they are spontaneously flattened over the supporting carbon film. For larger particles, ultra-microtome cuts are used, [21] to observe the elemental distribution in the particle bulk.

This technique produced some unexpected results. For instance, in many types of latex the sulfur elemental map shows this element distributed across the particle bulk but depleted in the surface. Since sulfur is found as sulfate or sulfonate from initiator residues or surfactant, these particles have negative charges throughout their interior. On the other hand, the sodium and potassium counter-ions are often observed in a narrow shell surrounding the particle, but in other cases they appear spread throughout the whole particle volume. This means that most dry latex particles have a negative core and a positive shell. Moreover, since the charge distributions are not highly symmetric, the particles are electric multipoles, and the domains with excess positive or negative charges extend for many tens and even hundreds of nanometers.

More recently, rather complex elemental distribution patterns have been observed, as shown in Figure 4. These elemental maps are from a submonolayer of the same particles presented in Figure 2. The individual particles are strongly deformed and flattened over the supporting carbon film, allowing the observation of a strong accumulation of P and thus of the phosphate groups bearing negative charges, at the particle borders. These P-rich domains are also electron-dense, since they are observed as very dark spots in the bright-field image. On the other hand, they appear as darker areas in the carbon elemental map, showing that they have a low carbon content relative to the particle bulk. O is distributed throughout the particles, since it is largely associated with the acrylic monomer.

Spectroscopy imaging in the transmission microscope is a *transmission* technique; consequently the images show the presence of an element throughout the whole sample thickness, provided the sample is sufficiently thin to allow for the escape of a few inelastic

scattered electrons. In another frequent pattern, sulfur (and thus the negative sulfate groups)

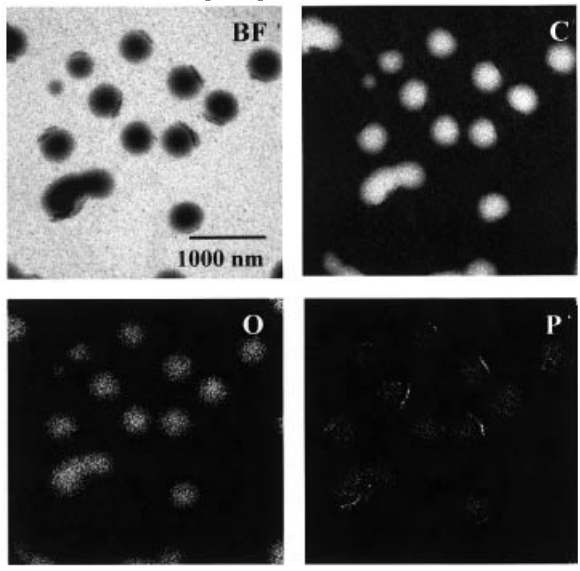


Figure 4. Bright-field (BF) picture and elemental (carbon, C; oxygen, O; phosphorus, P) maps of a poly(styrene-co-butyl acrylate-co-acrylic acid) latex ($T_g$=15°C).

is unevenly distributed throughout the whole particle, as shown in the elemental maps for a polystyrene latex in Figure 5.

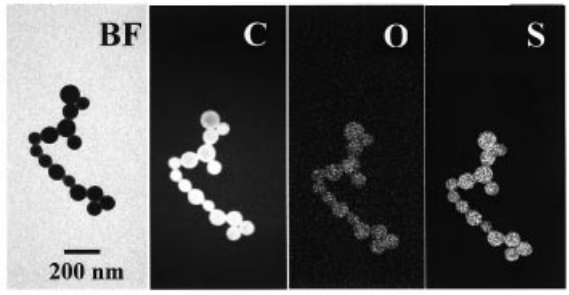


Figure 5. Bright-field picture and elemental maps of a poly(styrene) latex. This is the same latex presented in Fig. 1.

## Charge mapping in thermoplastics

A previous work[1] presented electrical distribution maps for a variety of common thermoplastics, and this was later observed also in the case of plasticized cellulose acetate membranes prepared following a phase-inversion procedure [22] (Figure 6).

Understanding the large electric potential gradients in the cellulose acetate, polyolefin and other SEPM pictures is not as easy as in the case of the latexes, because they cannot be associated to local excess of ionic charge. The acetylated cellulose can bear a few carboxylic groups arising from cellulose oxidation, but cellulose acetate membranes are well known for their low adsorption ability, which makes them highly suitable for the handling of proteins and other biological materials. This low adsorption ability is in turn evidence for the absence or a very low concentration of ionic groups, in the membrane surface. Consequently the large observed electric potential gradients can hardly be assigned solely to the oxidized cellulose residues.

Before raising other hypotheses, it should be recalled that the species responsible for charge separation have not yet been properly described, regardless if Maxwell or Costa Ribeiro effects is concerned.

A possible explanation for the charge separation in cellulose acetate membranes is based on the well-known ability of hydrophobic surfaces for differential adsorption of $H^+$ and $OH^-$ ions, with an advantage to the later. Consequently, the more hydrophobic surface domains at the polymer surface during membrane casting could be loaded with hydroxyl ions, as opposed to the more hydrophilic domains, thus creating spots with negative potential. Other possible explanations are the electro-kinetic phenomena associated to mass transfer during film casting, *e.g.* streaming potentials and junction potentials. These are usually less than 100 mV when the polymer is highly swollen with water, but may reach much higher values upon drying, when the separated charges are trapped in liquid pools and finally they are rendered immobile.

Still another possibility for charge separation arises from tribochemistry [23]: chain rupture in the stressed quasi-dry membrane can be at least partly heterolytic, thus producing chain - bound ions. The demonstration of tribochemical free radical formation is rather easy by electron-spin resonance, but unfortunately the formation of ionic defects cannot be monitored by highly sensitive fast spectroscopic techniques, analogous to free radicals.

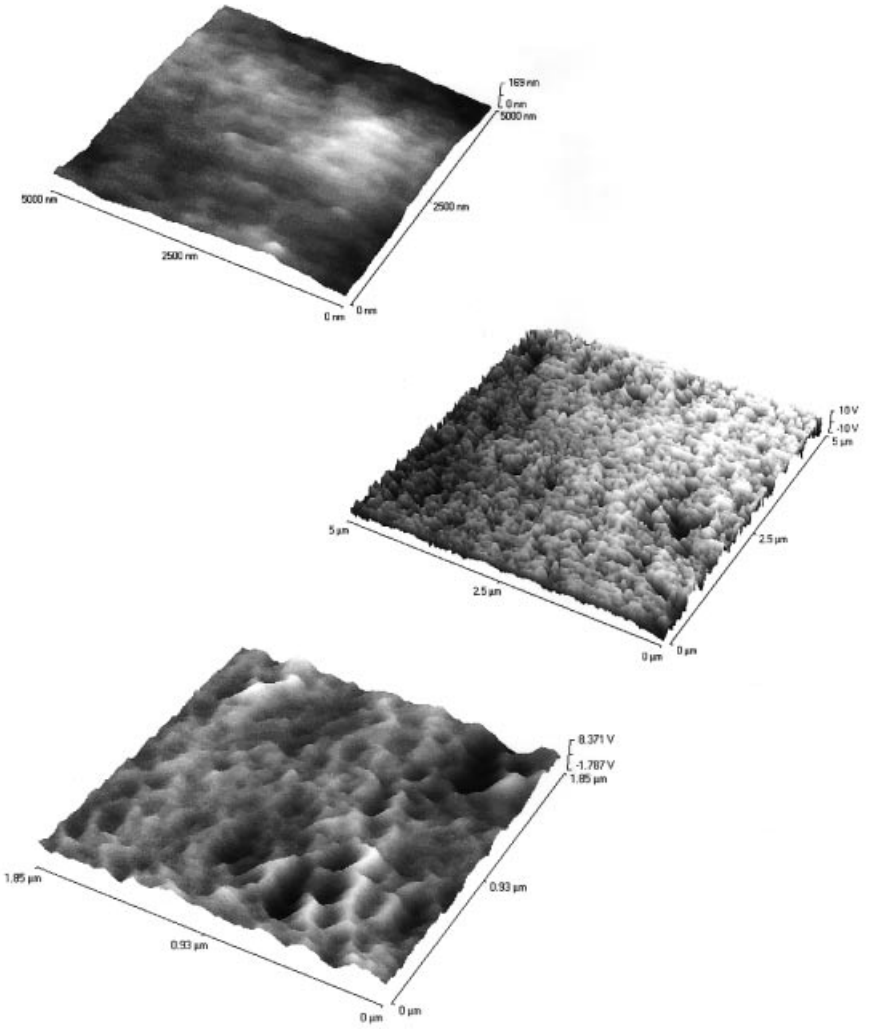


Figure 6. AFM (top) and SEPM (medium and bottom) images of a cast cellulose acetate membrane prepared by phase inversion and plasticized with glycerol, prior to drying and storage. Acquisition of the dry membrane images was not possible; so the membrane was wetted with $1.0 \times 10^{-3}$ mol $L^{-1}$ aqueous KCl, prior to the acquisition of these images.

It is important to verify the significance of local electric potentials experimentally determined close to film surfaces, by comparing them to the results of model calculations. This is being done in the authors' laboratory, by evaluating the local potentials generated by predefined distributions of electric charges. For instance, a 400-nm diameter disc with 176 equally spaced negative charges and surrounded by a 20-nm thick shell studded with 176 positive charges generates an electric potential map, measured 10 nm above the surface, well represented as a positive ring enclosing a negative disk. This is consistent with the images in Figures 1-3 and with the SEPM images for poly(styrene-co-hydroxyethylmetacrylate) films, published elsewhere.[1]

## Conclusion

Polymer films and particles are decorated with patterns of charged domains, as evidenced by new electric probe microscopy techniques, as well as by energy-loss analytical electron microscopy. Polymer colloidal particles and thin films charged domains are associated with the local concentrations of ionic groups, but the speciation of charge-bearing groups in cellulose acetate and other common thermoplastics has not yet been achieved, and it will depend on the combination of electric probe microscopy with a spatially-resolved molecular spectroscopy, perhaps near-field Raman imaging.

The mosaic of positive and negative electric potentials detected just above the polymer surface proves the existence of an electric charge mosaic within the polymer. This charge distribution is not explicitly recognized in the current polymer literature, and some currently widespread assumptions and models are actually in disagreement with the experimental data presented in this paper.

For these reasons, future work will have three major aims:

i) evaluation of the effect of excess charges on polymer mechanical, optical, permeation, adhesion and chemical properties.

ii) identification of other species beyond simple ions, in the domains with different local charges, probably by using near-field Raman spectroscopy.

iii) use of this new information on charged sites in polymers, to develop new polymer materials.

Acknowledgements: AJK, ETN, MB and MMR are graduate fellows from Fapesp. FG acknowledges support from CNPq, Fapesp, Pronex/Finep/MCT, and the Serrana company. This is a contribution of Millenium Institute for Complex Materials (PADCT/MCT).

[1] A. Galembeck, C. A. R. Costa, M. C. V. M. Silva, E. F. Souza, F. Galembeck, *Polymer* **2001**, *42*, 4845.
[2] K. Wu, M. J. Iedema, J. P. Cowin, *Science* **1999**, *286*, 2482.
[3] S. Bauer-Gogonea, R. Gerhard-Multhaupt, *IEEE Trans Dielectr Electr Insul* **1996**, *3*, 677.
[4] J. A. Malecki, *Phys Rev B* **1999**, *59*, 9954.
[5] C. Lacabanne, P. Goyaud, R. F. Boyer, *J Polym Sci* **1980**, *18*, 277.
[6] K. Shrivastava, J. D. Ranade, A. P. Srivastava, *Thin Solid Films* **1980**, *67*, 201.
[7] M. Mudarra, J. Belana, J. C. Cañadas, J. A. Diego, *Polymer* **1999**, *40*, 2569.
[8] S. M. Skinner, R. L. Svage, J. E. Rutzler Jr, *J Appl Phys* **1953**, *24*, 438.
[9] S. M. Skinner, *J Appl Phys* **1955**, *26*, 509.
[10] J. C. Ribeiro, *An Acad Bras Cienc* **1950**, *22*, 325.
[11] P. Eyerer, *Adv Colloid Interface Sc* **1972**, *3*, 223.
[12] D. Rollik, S. Bauer, R. Gerhard-Multhaupt , *J. Appl Phys* **1999**, *85*, 3282.
[13] B. D. Terris, J. E. Stern, D. Rugar, H. J. Mamin, *J Vac Sci Technol A-Vac Surf Films* **1980**, *8*, 374.
[14] M. Nonnenmacher, M. P. O'Boyle, H. K. Wickramasinghe, *Appl Phys Lett* **1991**, *58*, 2921.
[15] F. Saurenbach, B. D. Terris, *Appl Phys Lett* **1990**, *56*, 1703.
[16] W. F. Schmidt, "*Liquid State Electronics of Insulating Liquids*", CRC Press, Boca Raton NY **1997**.
[17] F. Galembeck, C. A. R. Costa, A. Galembeck, M. C. V. M. Silva, *An Acad Bras Cienc* **2001**, *73*, 495.
[18] J. M. Moita-Neto, V. A.R. Monteiro, F. Galembeck, *Colloids Surf A* **1996**, *108*, 83.
[19] M. Braga, C. A. R. Costa, C. A. P. Leite, F. Galembeck, *J Phys Chem B* **2001**, *105*, 3005.
[20] A. J. Keslarek, C. A. R. Costa, F. Galembeck, *Langmuir* **2001**, *17*, 7886.
[21] A. H. Cardoso, C. A. P. Leite, F. Galembeck, *Langmuir* **1998**, *14*, 3187.
[22] S. P. Nunes, F. Galembeck, *J Polym Sci Part C - Polym Lett* **1983**, *21*, 49.
[23] G. Heinicke, "*Tribochemistry*", Hanser, Berlin **1984**.